

Electron momentum spectroscopy of the HOMO of acetone

Tae Kyung Cho, Masahiko Takahashi*, Yasuo Udagawa

Institute of Multidisciplinary Research for Advanced Materials, Tohoku University, Katahira 2-1-1, Sendai 980-8577, Japan

Available online 28 November 2005

Abstract

Electron momentum profiles of the highest occupied molecular orbital (HOMO) of acetone have been measured under experimental conditions where a use of the plane-wave impulse approximation is justified. A double peak is observed in the experimental profile and it was found that calculated profiles by the use of the standard basis set always underestimate the magnitude of the low-momentum peak. Possible origins of the discrepancies between the calculated and measured profiles are examined, leading to an improved agreement by modifying the exponents of diffuse functions employed.

© 2005 Elsevier B.V. All rights reserved.

Keywords: Electron momentum spectroscopy; Momentum profile; Acetone

1. Introduction

The key to understanding the chemical properties of molecules is a detailed knowledge of electron behavior, most importantly for the electrons in the outermost valence orbital. Quantum chemical calculations have been extensively carried out to achieve this goal and electron density distribution in position space is one of the most useful concept in such studies. Electron momentum spectroscopy (EMS) [1–3], based on the binary ($e, 2e$) reaction, greatly helps us to understand electronic structure from a different point of view, i.e. from momentum space. The EMS experiment basically provides two types of information. First, binding energy spectra are obtained over a wide energy range, for example, by scanning the incident electron energy while detecting in coincidence the two emitted electrons having a fixed energy. Second, spherically averaged electron momentum distribution or momentum profile for individual orbitals in atoms and molecules are obtained by measuring the EMS cross-section at a fixed value of the binding energy as a function of the azimuthal angle difference between the two emitted electrons. While binding energy spectra are similar to those obtained by photoelectron spectroscopy, momentum distribution is unique to EMS. It is extremely sensitive to the low-momentum part, which corresponds to the chemically important

outer spatial regions of valence orbital electron density in the position space.

Earlier EMS studies employing single-channel detection systems were, however, plagued by low cross-sections and the resultant momentum distributions were qualitative rather than quantitative. Recent developments in multi-channel detection technique have significantly improved the quality of experimental data. At the same time, thanks to advancements in computational technology, extensive theoretical calculations with large basis sets have now become easily accessible. As a consequence, a great deal of theoretical and experimental EMS studies has been made on many orbitals of a variety of molecules to find good agreement between them [4].

There still exist, however, a number of orbitals for which theoretical calculations fail to reproduce observed momentum profiles, in particular at low-momentum region [5–10]. One of the notable examples is the highest occupied molecular orbital (HOMO) of acetone. Acetone is the prototype molecule for aliphatic ketones and plays fundamental roles in photochemistry and photobiology; its photochemical decomposition, initiated by the excitation of the HOMO electron to the lowest unoccupied molecular orbital (LUMO), is one of the most thoroughly studied organic photoreaction [11]. EMS study on the HOMO of acetone was first carried out by Brion and coworkers with the use of a single-channel spectrometer [7]. Because the accuracy and statistics of the experimental data were limited due to the low cross-section of this orbital, the acetone molecule was chosen as the first target when a multi-channel EMS spectrometer was con-

* Corresponding author. Tel.: +81 22 217 5386; fax: +81 22 217 5337.
E-mail address: masahiko@tagen.tohoku.ac.jp (M. Takahashi).

structed by the same research group [8]. Although a particularly detailed study was made on the HOMO with much improved experimental accuracy, large discrepancies were found to exist between the experimental momentum distribution obtained at impact energy of 1200 eV and all the calculated ones including CI calculations with very large basis sets.

In a recent study, it was found that experimental momentum distributions of some orbitals show remarkable orbital-dependent impact energy dependences [10], and hence it was suggested that a use of the plane-wave impact approximation (PWIA), which is assumed in most EMS studies, may not always be justified for polyatomic molecules. The impact energies employed in most EMS studies, around 1200 eV, may not be high enough to warrant the use of the PWIA.

In this study, electron momentum profile of the HOMO of acetone is thoroughly studied with varying impact energy and compared with various calculations. It was found that for this orbital the high-energy limit is reached at impact energy of 1200 eV but still discrepancies exist between experimental momentum profile and calculated ones by conventional basis sets. Possible origins of the discrepancies are examined and concluded to be resolved by changing functional forms of diffuse functions in the standard basis sets.

2. Experimental method and theoretical calculations

EMS is a high-energy electron-impact ionization experiment in which the kinematics of all the electrons are fully determined. In the symmetric non-coplanar scattering geometry, two outgoing electrons having equal energies and making equal polar angles of 45° with respect to the incident electron beam are detected in coincidence. Then, the magnitude of the target electron momentum before collision can be determined by measurements of the out-of-plane azimuthal angle difference between the two outgoing electrons. The EMS spectrometer employed has been previously described in detail [12]. Briefly, it consists of an electron gun, a set of electrostatic lens system, a spherical analyzer and a pair of position-sensitive detectors. Acetone from Tokyo Kasei was degassed by repeated freeze–pump–thaw cycles before use. The experiments were carried out at impact energies of 800, 1200 and 1600 eV. To achieve higher energy resolution the electrons were energy-analyzed and detected after being decelerated to 4:1 with the electrostatic lens system. The instrumental energy and momentum resolutions were then about 1.68, 1.71 and 2.33 eV (FWHM) and about 0.16, 0.19 and 0.21 a.u. at impact energies of 800, 1200 and 1600 eV, respectively. No detectable impurities were observed in the binding energy spectra.

Within the PWIA the EMS cross-section σ_{EMS} for a gaseous target is given by:

$$\sigma_{\text{EMS}} \propto \int \left| \left\langle \mathbf{p} \psi_f^{N-1} \middle| \psi_i^N \right\rangle \right|^2 d\Omega_p. \quad (1)$$

Here, ψ_i^N and ψ_f^{N-1} are the initial neutral (N electron) and final ionic ($(N-1)$ electron) wavefunctions, and \mathbf{p} is a plane wave representing the target electron at the collision instant. The target

Kohn–Sham (KS) approximation has been proposed as a means of approximating Dyson orbitals by KS orbitals [13–15]. With these approximations Eq. (1) is reduced to:

$$\sigma_{\text{EMS}} \propto \int |\psi_j(\mathbf{p})|^2 d\Omega_p, \quad (2)$$

where $\psi_j(\mathbf{p})$ is the j th one-electron momentum–space orbital.

Theoretical momentum profiles have been calculated by density functional theory (DFT) using the B3LYP functional [16]. Briefly, position–space wavefunctions of the molecules were generated using the Gaussian03 program and were subsequently converted to momentum profiles with the aid of the HEMS program developed by Brion and coworkers. To compare with experiments all the profiles were folded with the instrumental momentum resolution according to Migdall et al. [17].

The molecular structure of acetone has been determined from microwave spectroscopy and electron diffraction as follows: four heavy atoms and two hydrogen atoms are in the same plane, and the in-plane hydrogen atoms eclipse the oxygen [18–20]. Assuming this conformation (C_{2v}) geometry optimization calculation was made by the DFT method applying the B3LYP functional by the use of the 6-31G** basis set and the geometrical parameters thus obtained are used to calculate σ_{EMS} . Contributions from some other possible conformers are also examined as will be described later.

3. Results and discussion

3.1. Binding energy spectra

Binding energy spectra of acetone in the range 5–18 eV measured at impact energies of 800, 1200 and 1600 eV are shown in Fig. 1. The spectra were obtained by summing all the coincidence signals over the entire azimuthal angle difference range covered. From photoelectron spectroscopy studies [21,22] five orbitals are known to exist below 15 eV: $5b_2$ (9.8 eV), $2b_1$ (12.6 eV), $4b_2$ (\sim 13.4 eV), $8a_1$ (14.1 eV) and $1a_2$ (\sim 14.4 eV). Deconvolution of low-energy part of each spectrum was attempted by using three Gaussians centered at 9.8, 12.6 and \sim 14 eV. The deconvoluted curves thus obtained are shown as dotted curves and their sum as a solid curve in the figure. Although the energy of the third Gaussian peak is somewhat ambiguous, it will be evident that it does not affect the intensity of the Gaussian curve attributed to the HOMO thus extracted. A similar fitting procedure was employed for a series of binding energy spectra at each azimuthal angle difference. Then, experimental momentum profiles at each impact energy were produced by plotting the area of the Gaussian curves of the HOMO as a function of azimuthal angle difference.

3.2. Impact energy dependence of momentum profile

Since the experimental momentum profiles or cross-sections are not absolute, the results under different experimental conditions must be normalized when comparisons are made. In this

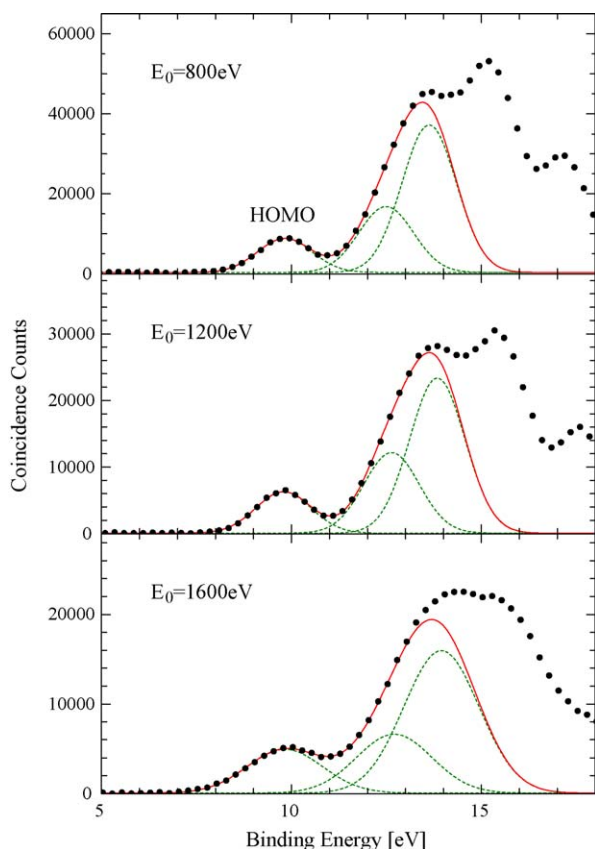


Fig. 1. Solid circles are binding energy spectra of acetone, measured at impact energies indicated in the figure. Dotted curves are Gaussian deconvolution curves and solid curves are their sum.

study, each momentum profile was normalized by the use of Eq. (3).

$$\int |\psi_j(\mathbf{p})|^2 d\mathbf{p} = 1 \quad (3)$$

Fig. 2 shows experimental momentum profile of the HOMO obtained at impact energies of 800, 1200 and 1600 eV. Here, an integrand from 0 to 2.0 a.u. was employed. Almost the same

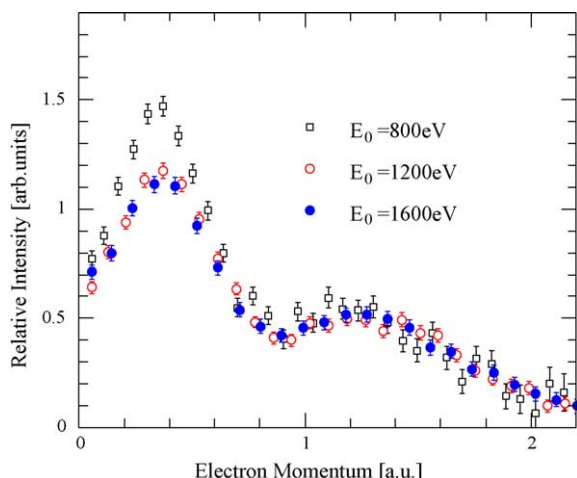


Fig. 2. Impact energy dependence of momentum profile of acetone HOMO.

results were obtained by the use of somewhat different integrand, for example, from 0 to 1.75 or 2.25 a.u.

An existence of a double peak at about 0.4 and 1.3 a.u. is characteristic of the momentum profile of this orbital, as has been observed in the previous studies [7,8]. The relative intensity of the two peaks, however, depends on impact energy; the low-momentum peak reduces with the increase in impact energy from 800 to 1200 eV. On the other hand, the momentum profile remains almost unchanged with an increase in impact energy from 1200 to 1600 eV. Apparently PWIA does not hold for the HOMO of acetone at the impact energy of 800 eV, while 1200 eV impact energy is enough to ensure a use of PWIA.

This is in contrast with earlier impact energy dependence studies of momentum profiles for atoms and simple diatomic molecules such as noble gases [23–26], H₂ [27], HF [28–30] and CO [31], but in parallel with the recent observation for polyatomic molecules glyoxal and biacetyl [10]. In passing, it may be worthwhile to mention that impact energy dependence of electron momentum profile even above 1200 eV seems to be not an exception for relatively large molecules; in a separate experiment on an analogous molecule acetaldehyde it was also found that momentum profile changes up to impact energy of 1600 eV, but remains the same at impact energy of 2000 eV [32]. The results obtained here support the assertion that the range of validity of the PWIA depends on the target and care has to be exercised for the use of PWIA [10].

Now a use of the PWIA is ensured for the momentum profile of acetone HOMO obtained at impact energy above 1200 eV, we can compare the momentum profile at 1200 or 1600 eV with the PWIA calculations. Fig. 3 shows the momentum profile obtained at impact energy of 1600 eV together with theoretical momentum profiles generated by the DFT using several standard basis sets indicated in the figure. Normalization is also made for theoretical momentum profiles by the use of Eq. (3). Even the smallest basis set shown in the figure, 6-31G, reproduces the observed double peak, but significantly underestimates the height of the first peak of the experimental data.

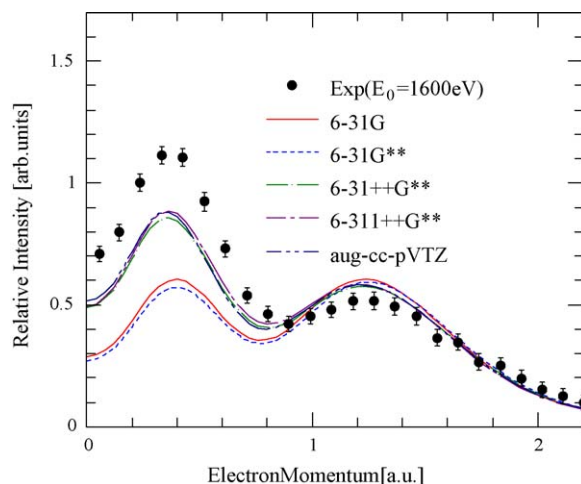


Fig. 3. Comparison of experimental momentum profile of acetone HOMO obtained at impact energy of 1600 eV (solid circles) and theoretical ones by using basis sets indicated in the figure.

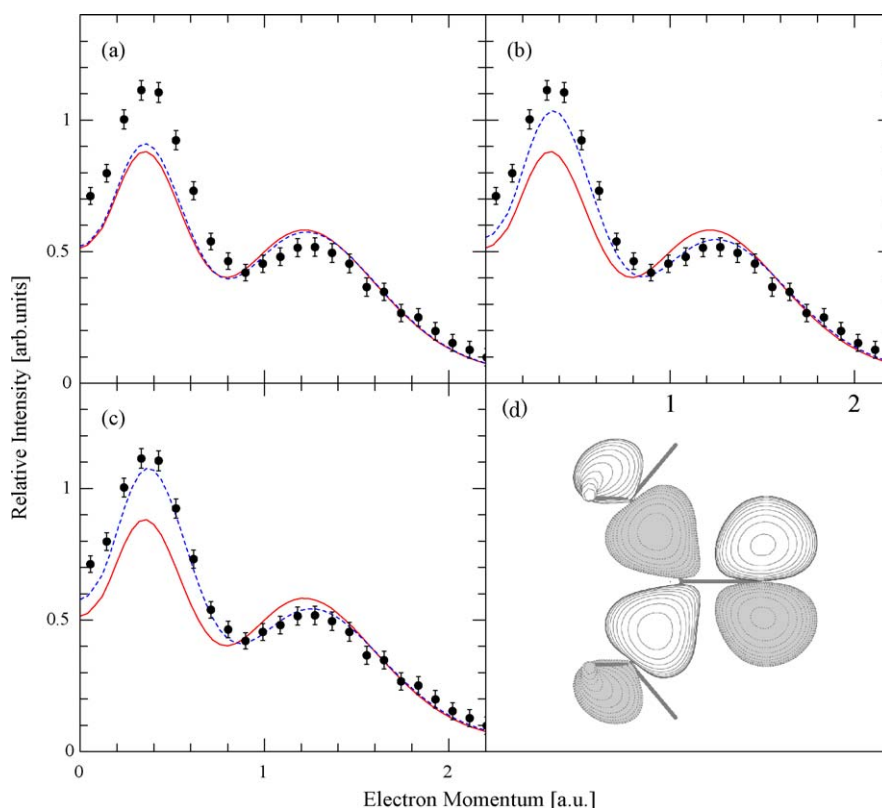


Fig. 4. Comparison of the calculated momentum profiles without (solid curve)/with (dots) reduction of the exponent of diffuse function by a factor of 2. Experimental momentum profile is also shown by solid circles. (a) C 2p, (b) O 2p, (c) O 2p + C 2p + H 2p and (d) electron density distribution of acetone HOMO calculated with aug-cc-pVTZ.

An addition of polarization function, 6-31G**, shows almost no improvement in the fit. On the other hand, better agreement with the experimental data can be achieved by an addition of diffuse functions. All the three basis sets incorporating diffuse functions, 6-31++G**, 6-311++G** and aug-cc-pVTZ, show almost indistinguishable momentum profiles with each other, but still considerably underestimate the first peak. A use of more extended basis set, aug-cc-pVQZ, gives almost the same results. In short, even with much improved accuracy in experimental data than that previously obtained [7,8], the discrepancies between theoretically calculated momentum profiles and the experimentally observed one could not be resolved. Since experimental momentum profile does not change at impact energies above 1200 eV, a failure of PWIA cannot be the reason of the discrepancies. In what follows implications of the observed apparent discrepancies is discussed.

Two possible origins of the discrepancies related to nuclear positions can be conceived; molecular conformation and low-frequency vibration. Orientation of methyl group has been reported to have almost no effect on the momentum profiles of dimethyl ether [5,6] and biacetyl [10]. In a recent publication, however, Deleuze et al. [33] observed about *n*-butane that significant differences in the momentum profiles exist between the all-staggered and the gauche forms. In the case of acetone, in addition to the eclipse–eclipse conformation described in Section 2, several other stable conformers such as staggered–staggered and staggered–eclipse are possible.

Momentum profiles were calculated about seven possible conformers after structure optimization, and we did find that momentum profiles depend considerably on conformation. In particular, the momentum profile of the staggered–staggered conformer shows much higher low-momentum peak which roughly reproduces the experimental one. However, an ab initio study combined with spectroscopic data by Smeyers et al. [34] indicates that the total energy of this conformer is higher than the most stable eclipse–eclipse form by over 700 cm^{−1}, which was confirmed by our independent calculations. Hence, the contribution of the staggered–staggered conformer to experimental momentum profile must be negligible at room temperature. Combining calculated profiles with Boltzmann distribution factors for other possible conformers, we conclude that presence of several other conformers cannot explain the observed discrepancies between experimental and calculated momentum profiles.

In addition to methyl torsional motion, the acetone molecule has a low-frequency CO out-of plane bending vibration. The frequency is reported to be 124.5 cm^{−1}; low enough to make some contribution at room temperature [35]. It was found from calculations, however, that electron momentum profile hardly depends on the out-of-plane coordinate of the oxygen atom, and hence the possibility from excited out-of-vibration mode is ruled out.

Since consideration of molecular conformation and molecular vibration cannot resolve the discrepancies between the experiment and theoretical calculations, the origin of the difference

should be sought for in electronic state calculations. Because all the calculations underestimate the ionization intensity in the low-momentum region that corresponds to electron distribution in the outer spatial region, it is natural to suspect that the diffuse functions employed in the conventional basis sets may not be diffuse enough. Hence, calculations were carried out by varying the exponents of diffuse functions of the carbon and oxygen atoms. The HOMO of acetone, which is depicted in Fig. 4d, is mainly due to the lone-pair oxygen 2p electrons with fairly large contribution from the methyl group carbons and hydrogens. Because of the b_2 symmetry of the HOMO oxygen 2s orbital is not involved. Hence, calculations were carried out by changing the exponents of the diffuse functions of oxygen 2p, carbon 2s and 2p, and hydrogen 1s and 2p, which are included in the aug-cc-pVTZ basis functions. It turned out that reducing the exponents of hydrogen 1s, carbon 2s and 2p into halves or less makes only slight changes on the momentum profile. As an example, the momentum profile calculated when the exponent of the carbon 2p diffuse function is reduced by a factor of 2 is shown in Fig. 4a together with that calculated using the standard basis set. The difference is discernible, but only barely.

On the other hand, as is expected from the constituents of the HOMO, reducing the exponents of oxygen 2p by a factor of 2 makes significant changes, as is shown in Fig. 4b; the first peak increases, and the second one decreases considerably, approaching the experimentally observed profile. Reduction of the exponents less than half makes almost no change. When the exponents of the 2p diffuse functions of oxygen, carbon and hydrogen are reduced by a factor of 2, the calculated momentum profile almost coincides with the observed one, as is evident from Fig. 4c. That is, the HOMO orbital of acetone is spatially more diffuse than anticipated so far.

It is interesting to note that calculation always underestimate the magnitudes of the low-momentum region when large discrepancies between calculations and observations are reported [5–10]. In all these studies, it has been confirmed that incorporation of conventional diffuse functions makes calculated momentum profiles closer to the observed ones. It may be worthwhile to re-examine those orbitals along the lines employed in this study.

References

- [1] E. Weigold, I.E. McCarthy, *Electron Momentum Spectroscopy*, Kluwer Academic/Plenum Publishers, New York, 1999.
- [2] C.E. Brion, *Int. J. Quantum Chem.* 29 (1986) 1397.
- [3] M.A. Coplan, J.H. Moore, J.P. Doering, *Rev. Mod. Phys.* 66 (1994) 985.
- [4] C.E. Brion, G. Cooper, Y. Zheng, I.V. Litvinyku, I.E. McCarthy, *Chem. Phys.* 13 (2001) 13.
- [5] S.A.C. Clark, A.O. Bawagan, C.E. Brion, *Chem. Phys.* 137 (1989) 407.
- [6] Y. Zheng, E. Weigold, C.E. Brion, W. von Niessen, *J. Electron. Spectrosc. Relat. Phenom.* 53 (1990) 153.
- [7] B.P. Hollebone, P. Duffy, C.E. Brion, Y. Wang, E.R. Davidson, *Chem. Phys.* 178 (1993) 25.
- [8] Y. Zheng, J.J. Neville, C.E. Brion, Y. Wang, E.R. Davidson, *Chem. Phys.* 188 (1994) 109.
- [9] Y. Zheng, J. Rolke, G. Cooper, C.E. Brion, *J. Electron. Spectrosc. Relat. Phenom.* 123 (2002) 377.
- [10] M. Takahashi, T. Saito, J. Hiraka, Y. Udagawa, *J. Phys. B: At. Mol. Opt. Phys.* 36 (2003) 2539.
- [11] Y. Haas, *Photochem. Photobiol. Sci.* 3 (2003) 6.
- [12] M. Takahashi, T. Saito, M. Matsuo, Y. Udagawa, *Rev. Sci. Instrum.* 73 (2002) 2242.
- [13] P. Duffy, D.P. Chong, M.E. Casida, D.R. Salahub, *Phys. Rev. A* 50 (1994) 4707.
- [14] M.E. Casida, *Phys. Rev. A* 51 (1995) 2005.
- [15] P. Duffy, *Can. J. Phys.* 74 (1996) 763.
- [16] A.D. Becke, *J. Chem. Phys.* 98 (1993) 5648.
- [17] J.N. Migdall, M.A. Coplan, D.S. Hensch, J.H. Moore, J.A. Tossell, V.H. Smith Jr., J.W. Liu, *Chem. Phys.* 57 (1981) 141.
- [18] R. Nelson, L. Pierce, *J. Mol. Spectrosc.* 18 (1965) 344.
- [19] T. Iijima, M. Kimura, *Bull. Chem. Soc. Jpn.* 42 (1968) 2159.
- [20] T. Iijima, *Bull. Chem. Soc. Jpn.* 45 (1972) 3526.
- [21] G. Bieri, L. Asbrink, W. von Niessen, *J. Electron. Spectrosc. Relat. Phenom.* 27 (1982) 129.
- [22] K. Kimura, S. Katsumata, Y. Achiba, I. Yamazaki, S. Iwata, *Handbook of HeI Photoelectron Spectra of Fundamental Organic Molecules*, Japan Scientific Society, Tokyo, 1981.
- [23] E. Weigold, S.T. Hood, P.J.O. Teubner, *Phys. Rev. Lett.* 30 (1973) 475.
- [24] S.T. Hood, I.E. McCarthy, P.J.O. Teubner, E. Weigold, *Phys. Rev. A* 8 (1973) 2494.
- [25] S.T. Hood, I.E. McCarthy, P.J.O. Teubner, E. Weigold, *Phys. Rev. A* 9 (1974) 260.
- [26] M.J. Brunger, I.E. McCarthy, E. Weigold, *Phys. Rev. A* 59 (1999) 1245.
- [27] S. Dey, I.E. McCarthy, P.J.O. Teubner, E. Weigold, *Phys. Rev. Lett.* 34 (1975) 782.
- [28] C.E. Brion, I.E. McCarthy, I.H. Suzuki, E. Weigold, *Chem. Phys. Lett.* 67 (1979) 115.
- [29] C.E. Brion, S.T. Hood, I.H. Suzuki, E. Weigold, G.R.J. Williams, *J. Electron. Spectrosc. Relat. Phenom. J. Electron. Spectrosc.* 21 (1980) 71.
- [30] S.W. Braidwood, M. Brunger, D.A. Kononov, E. Weigold, *J. Phys. B: At. Mol. Opt. Phys.* 26 (1993) 1655.
- [31] S. Dey, A.J. Dixson, K.R. Lassey, I.E. McCarthy, P.J.O. Teubner, E. Weigold, P.S. Bagus, E.K. Viinikka, *Phys. Rev. A* 15 (1977) 102.
- [32] T.K. Cho, M. Takahashi, Y. Udagawa, unpublished result.
- [33] M.S. Deleuze, W.N. Pang, A. Salam, R.C. Shang, *J. Am. Chem. Soc.* 123 (2001) 4049.
- [34] Y.G. Smeyers, M.L. Senent, V. Botella, D.C. Moule, *J. Chem. Phys.* 98 (1993) 2754.
- [35] D.W. Liao, A.M. Mebel, M. Hayashi, Y.J. Shiu, Y.T. Chen, S.H. Lin, *J. Chem. Phys.* 111 (1999) 205, and references therein.